A PROPOSED COMPREHENSIVE MODEL FOR ELEVATED FLARE FLAMES AND PLUMES

David Shore
Flaregas Corporation, Nanuet. N.Y. 10954. U.S.A.
PH: 1-845-371-2519
davids@flaregas.com

Prepared for presentation at
American Institute of Chemical Engineers
2006 Spring National Meeting
40th Annual Loss prevention Symposium
Orlando, Florida
April 24 – 26, 2006

A PROPOSED COMPREHENSIVE MODEL FOR ELEVATED FLARE FLAMES AND PLUMES

David Shore
Flaregas Corporation, Nanuet. N.Y. 10954. U.S.A.
Ph: 1-845-371-2519
davids@flaregas.com

ABSTRACT

When designing elevated flares, the open flame and the associated radiant heat represent the most obvious safety considerations and several different flames models are available in the literature to aid in the design process on this basis.
An often overlooked consideration however is the effect of the flue gas plume itself and how this can impact plant safety in the near field due to its inherent temperature, reduced oxygen and potential concentration of unburned materials, affecting both personnel access areas and local structures.

Disadvantages of the commonly used flame models include

- a universal assumption that all flare discharges are axially vertical, rendering these models inaccurate in many Offshore and Oil field applications, and
- a discontinuity between the flame and downwind plume models, making it difficult to estimate near-field downwind effects.

This paper introduces a new algorithm for a flame model, referenced in the paper as the BUOYANT Flame Model, using the indicator BUO, which

- is based on widely used parameters for buoyant rise and momentum rise of a plume
- includes a vector component to allow use for both vertical or non-vertical discharges
- can be applied equally to the flame and the resulting plume as a comprehensive solution.

The paper expands on the published dispersion formulae to show how the model may be used to approximate downwind plume temperature and flue gas concentrations in a three dimensional field. The new model can be a spring-board to further research and includes a time based component which may have general applicability to all diffusion flames and assist in flare flame efficiency estimations.

1 BACKGROUND

1.1 THE NEED FOR MODELING

Elevated flares are used, primarily but not exclusively, in the Oil and Petrochemical Industries to dispose of high-volume flows of flammable gases, which arise as an excess quantity in some emergency condition. In general, the design condition for a Refinery Flare results from some accumulation of separate and individual events which is so great in comparison to the everyday condition that there is a significant and intrinsic over-design for the day-to-day use and, in many cases, the theoretical design case will never be achieved.
In contrast, other industries, such as Pharmaceuticals, Chemicals and Gas Treatment, have a need to relieve toxic or noxious chemicals at predetermined rates and on a regular basis. Often this design condition may result from a single, specific event, raising its probability and elevating the need for an accurate flame model.

1.2 EXISTING FLAME MODELS

The most commonly investigated aspect of design is the thermal emission from the open flame, which is used to help to set the height of an elevated flare. This calculation procedure is described in API RP-521[1], and requires the prediction of the wind-blown flame position in order to locate a pseudo-center for the assumed, quasi-spherical distribution of thermal radiation used in the common, point source model. Other radiant models are also used in the industry but all need an initial estimate of position for the wind-blown flame.

The two most common flame-shape models used in the industry may be referenced as the Brzustowski [2] model (BRZ) and the API, "simple" model (API). Although these standard flame models in RP-521 suffer from some inconsistencies, they seem to generate workable results for Refinery Flare height design but may be imperfect for critical applications needing accurate results. Unfortunately, they only model wind-blown flames from vertical discharges. On a global scale, there are many applications of flares which have an angled or horizontal discharge, and these cannot be adequately modeled using the standard RP-521 techniques, raising an obvious need for an alternate model which can be applied to these other discharge directions.

Other flame models are available but, like the BRZ model, tend to be associated with testing on the small scale. Recent investigations by Majeski et al [3] of this type have been influenced by the unsteady nature of the small wind blown flame. Most models attempt to incorporate buoyant and

momentum parameters into a single characteristic, and relate flame length as a function of diameter, mimicking the conventional jet theory applicable to small scale models. Both the Majeski paper and a well known work on fuel jets by Hottel[4] indicate that there are essentially two flow regimes for diffusion flames. In the case of the Hottel paper the flames appear to quickly transition out of the laminar regime as diameter (and flame size) increase allowing this not to be a factor for the large flames considered by this paper. The Majeki work covers ratios of outlet to wind velocity that are less than 1. This involves conditions in which downwash can occur.

Although there are already excellent computer modeling techniques available which describe the intricate flame-cell-level reaction chemistry of medium sized flames, most theoretical models are not easily applied to large scale flames. For general usage, practical flame models need to be described in common engineering units using properties which are widely available to the engineering community. True flare flames are frequently large with a sufficient energy output to minimize momentary effects of wind, and seem to display a length characteristic more scalable with heat release and thermal properties than diameter, as shown by Zukoski[5]. These flames are large enough to display differences based on momentum (or inertia) domination and thermal (buoyancy) domination, and have been separately classified in this manner by Gogolek et.al[6]. The cited discussions have demonstrated differences between inertia domination and thermal buoyant domination as well as introducing an additional category for "wake" domination, but have not combined the characteristics into a single model. This paper attempts to create such a link by utilizing a model which incorporates both buoyant and momentum characteristics.

1.3 PLUME CONSIDERATIONS

Gases relieved into Flares may sometimes contain toxic materials such as Hydrogen Sulfide, Mercaptans, Hydrogen Cyanide, Ammonia and other similar materials. When these gases are burned in a flare, the design of the discharge height must take into consideration the possible downwind concentrations of pollutants, which may arise either

- as unburned materials released if the flame is extinguished,
- as unburned materials from inefficient combustion, or
- as products of combustion.

Downwind concentrations of pollutants in an airborne plume may be predicted using the well-known and widely used Pasquill / Gifford[7] [8] dispersion formula, as shown by Turner[9], together with a series of empirical, downwind dispersion coefficients. The most common assessments

involve Ground Level Concentrations in the far field which are based on the vertical height achieved by the plume.

A frequently ignored aspect of pollution is the concentration of unburned gases or flue gases in the hot plume, locally to the flare, where such gases may be blown toward, and engulf other plant equipment requiring a treatment for the near field.

Also, downwind predictions of plume rise are generally developed from chimney plumes and the commonly used formulae frequently involve the use of a plume discharge temperature, which is difficult to assess for the plume from an open flame. This makes it difficult to have confidence in the normal models to generate a suitable plume condition for the dispersion calculations from a flare flame.

This paper also attempts to address these features within a comprehensive treatment of the dispersion and plume rise modeling parameters.

2 FLAME RESIDENCE

2.1 DEVELOPING A REALISTIC RELATIONSHIP

The aspect of primary interest in the determination of any flame model must be the flame residence time t_F. To develop a relationship for time t_F, we can use the standard dispersion formulae as a guide.

When gases are ejected from a source such as a stack, they are diluted during subsequent down wind travel. According to the Pasquill/Gifford approach, this downwind dilution (on the plume centerline) can be expressed as

$$\frac{\chi \times U_A}{w_O} = \frac{1}{2 \times \pi \times \sigma_Y \times \sigma_Z} \qquad \textbf{Equation 2.1}$$

where χ = downwind concentration (normally as mass per unit volume)

U_A = mean wind speed through the plume

w_O = discharged mass flow rate

π = circular constant **= 3.14159.....**

σ_Y = horizontal dispersion coefficient

σ_Z = vertical dispersion coefficient

$\sigma_Y \times \sigma_Z$, the product of the dispersion coefficients, may be re-expressed as

$$\sigma_Y \times \sigma_Z = S \times X^N = S \times U_A{}^N \times t^N \qquad \textbf{equation 2.2}$$

where S = general dispersion constant

N = general dispersion exponent

t = elapsed time after discharge

X = downwind travel $= t \times U_A$ **equation 2.3**

In normal usage, the downwind dispersion formula anticipates ground reflection of the plume and the distribution occurs over a total perimeter of 2π radians. The centerline condition usually contains both the direct and reflected components. In the near field, before the plume has the opportunity to reach the ground the reflected components are absent. This allows the definition

atmospheric stability parameter $$K_S = \frac{1}{2 \times \pi \times S} \qquad \textbf{equation 2.4}$$

The downwind concentration is an expression of dilution of gas in air. In the case of downwind dilution of the flame, the mass flow rate can be replaced by the energy flux of the flame, q_F, and the concentration is replaced by the active energy density in the flame. This latter term can be represented by the limit state of thermal energy transfer which will sustain a flame by normal propagation and defined as K_F which is essentially the volumetric calorific value at the lean limit. This is similar to the temperature parameter developed by Pohl et al[10] when correlating flame lengths in the EPA flare studies but it accounts for the low limit concentration rather than the stoichiometric concentration used in the Pohl analysis.

Flame reactivity parameter $$K_F = CV \times \rho_O \times C_L \qquad \textbf{equation 2.5}$$

where CV = calorific value of the gas (mass basis)

ρ_O = density of discharged gas

C_L = Lean Limit Flammability concentration of discharged gas in air

2.2 FLAME DWELL-TIME FORMULA

Substituting all of the above values and rearranging the various formulae gives

$$t_F{}^N = \left(\frac{1}{2\times\pi\times S}\right)\times\left(\frac{1}{CV\times\rho_O\times C_L}\right)\times\left(\frac{1}{U_A{}^{(1+N)}}\right) \qquad \textbf{equation 2.6}$$

or, flame dwell time $$t_F = \left[\, q_F \times \left(\frac{K_S}{K_F}\right)\times\left(\frac{1}{U_A{}^{(1+N)}}\right)\right]^{\frac{1}{N}} \qquad \textbf{equation 2.6.1}$$

where q_F = heat flux of the flame

An interesting outcome of this relationship for t_F is the substitution for down wind distance to the end of the flame as

$$X_F = t_F \times U_A = \left[\, q_F \times \left(\frac{K_S}{K_F}\right)\times\left(\frac{1}{U_A}\right)\right]^{\frac{1}{N}} \qquad \textbf{equation 2.7}$$

which suggests a reduction in downwind travel as wind speed increases. This is an observed characteristic of flames and is illustrated by the research of Majeski et.al.

3 PLUME RISE

3.1 THE BRIGGS MODEL

The most commonly accepted plume model in use today is that developed by Briggs[11], which provides formulae describing the rise of plumes from stacks and chimneys. In general, Briggs' work is related to the final plume rise, which, most frequently, controls the downwind ground level concentrations of pollutants.

3.2 MODIFYING THE BRIGGS BUOYANCY PARAMETERS

Most plumes rise naturally because of their buoyant characteristics and the density differences in the air-diluted downwind plume of flue gas. Briggs provides a practical, plume rise solution, for

a buoyant plume from a chimney, based on the density differences between the discharged gas and the ambient air into which it discharges.

The rise or fall of a buoyant or dense plume from the point of discharge $= \Delta H_{P1}$

$$\Delta H_{P1} = \frac{K_B \times F_B^{\left(\frac{1}{3}\right)} \times X^{\left(\frac{2}{3}\right)}}{U_A} \qquad \textbf{equation 3.1.1}$$

where F_B = buoyancy parameter $= \left(1 - \frac{\rho_O}{\rho_A}\right) \times U_O \times r_O^{\,2}$ **equation 3.2**

K_B = buoyancy constant $= 1.6 \quad (Briggs)$

U_O = stack discharge velocity

U_A = mean wind speed through the plume

r_O = stack discharge radius

ρ_A = ambient air density

ρ_O = mean discharge density

The formula, as expressed above, is satisfactory when modeling raw gas discharge from a flare or vent. It yields positive buoyancy for light discharge and negative buoyancy for gases with a discharge density greater than air. It thus predicts that such gases will sink to grade from an elevated source. Although Briggs gives no comparable condition when developing the buoyant 'rise' formula, this case can be used to examine the possibility of finding flammable down-wind concentrations from a vent or an extinguished flare tip.

For a complete solution, the formula for ΔH_{P1} requires a good estimate of temperature for determination of discharge density. When dealing with an open Flare flame, such a determination can prove impractical. An adjustment of the formula, however, allows the use of the total thermal energy flux in the plume, which is clearly more appropriate for the flare than a solution requiring an estimation of bulk temperature, and is a good starting point for a new model involving a flame.

Thus we can re-define F_B as $F_H \times q$ **equation 3.3**

where $F_H = \frac{g}{\pi \times Cp \times T_A \times \rho_A}$ = thermal buoyancy parameter **equation 3.4**

q = thermal energy flux in plume

g = gravitational constant as required for consistent units

Cp = specific heat of the plume

T_A = ambient air temperature (abs)

which allows us to consider the rise of a hot, buoyant plume from the point of discharge = ΔH_{P2}

$$\Delta H_{P2} = \frac{K_B \times F_H^{\left(\frac{1}{3}\right)} \times q^{\left(\frac{1}{3}\right)} \times X^{\left(\frac{2}{3}\right)}}{U_A} \qquad \textbf{equation 3.1.2}$$

When applying this formula, we need to remember that a chimney plume has a fully developed heat content ***at the point of discharge*** whereas the heat from the flame develops over time ***after*** the gas leaves the discharge point. However, at any downwind location, the rate of dilution for either plume will be similar and the rate of rise will be a function of the developed heat at that point.

Looking, therefore, at the rate of rise of the buoyant plume leads to the following analysis.
By substitution of $X = t \times U_A$ and differentiation of the Briggs formula we can show that

$$\frac{dH}{dt} = \left(\frac{2 \times K_B}{3}\right) \times \left(\frac{F_H \times q}{U_A \times t}\right)^{\left(\frac{1}{3}\right)} \qquad \textbf{equation 3.5}$$

The downwind flame develops roughly according to a relationship based on the rate of air entrainment, which, in turn, is a function of local turbulence and rate of heat release.
Using the previously developed formula for the flame "dwell time", substituting for q, and reintegrating gives

$$t_F = \left[q_F \times K_N\right]^{\frac{1}{N}} \qquad \textbf{equation 2.6.3}$$

where $$K_N = \left(\frac{K_S}{K_F \times U_A^{(1+N)}}\right) \qquad \textbf{equation 3.6}$$

In the above equations, the buoyancy factor F_H may be modified to F_F to account for that radiated heat from the flame which does not contribute directly to a calculable plume rise. This is probably somewhat greater than the actual fraction of heat which reaches the ground and so a conservative reduction factor is applied here, based on the radiant losses.

$$F_F = F_H \times (1 - 1.5 \times \varepsilon) = \left(\frac{g}{\pi \times Cp \times T_A} \right) \times (1 - 1.5 \times \varepsilon) \qquad \textbf{equation 3.7}$$

ε = flame emissivity (radiated heat fraction)

from which

Flame rise $$\Delta H_F = \left[\frac{2 \times K_B}{(2+N)} \right] \times \left[\frac{F_F^{\left(\frac{1}{3}\right)}}{U_A^{\left(\frac{1}{3}\right)} \times K_N^{\left(\frac{1}{3}\right)}} \right] \times t^{\left(\frac{2+N}{3}\right)} \qquad \textbf{equation 3.1.3}$$

$$\Delta H_F = \left[\frac{2 \times K_B}{(2+N)} \right] \times \left[\frac{F_F^{\left(\frac{1}{3}\right)}}{U_A^{\left(\frac{3+N}{3}\right)} \times K_N^{\left(\frac{1}{3}\right)}} \right] \times X^{\left(\frac{2+N}{3}\right)} \qquad \textbf{equation 3.1.4}$$

3.3 INTERCHANGEABLE BUOYANT RISE EQUATIONS

The foregoing analysis provides ***three, interchangeable*** relationships for buoyant plume rise at distance X

for **raw gas plumes** with no combustion, based on non-thermal buoyancy in the original plume

$$\Delta H_{P1} = \frac{K_B \times F_B^{\left(\frac{1}{3}\right)} \times X^{\left(\frac{2}{3}\right)}}{U_A} \qquad \textbf{equation 3.1.1}$$

for **hot plumes** such as flue gas from chimneys, furnaces, incinerators, ground flares etc., and using fully developed thermal buoyancy in the plume

$$\Delta H_{P2} = \frac{K_B \times F_H^{\left(\frac{1}{3}\right)} \times q^{\left(\frac{1}{3}\right)} \times X^{\left(\frac{2}{3}\right)}}{U_A} \qquad \textbf{equation 3.1.2}$$

for an **open flame;** within the flame

$$\Delta H_F = \left[\frac{2 \times K_B}{(2+N)} \right] \times \left[\frac{F_F^{\left(\frac{1}{3}\right)}}{U_A^{\left(\frac{3+N}{3}\right)} \times K_N^{\left(\frac{1}{3}\right)}} \right] \times X^{\left(\frac{2+N}{3}\right)} \qquad \textbf{equation 3.1.4}$$

For an **open flame**; beyond the flame

$$\Delta H_{P3} = \Delta H_{P2} - \Delta H_E\{X_F\} \qquad \textbf{eq 3.8}$$

where $\Delta H_E\{X_F\} = \Delta H_{P2}\{X_F\} - \Delta H_{F1}\{X_F\}$ = height correction at X_F **eq 3.9**

X_F = horizontal end of the flame distance $= U_A \times t_F$ **eq 2.3.1**

ΔH_{P2} is evaluated using F_F

These latter formulae describe the conditions which predominate in flames categorized by **thermal dominance**.

3.4 INCORPORATING DISCHARGE MOMENTUM

The gases leaving the end of the stack also possess a certain momentum flux which contributes to the local position of the flame. Briggs also provides a formula for plume rise based on jet discharge which can be expressed as

$$\Delta H_M = K_M \times \left[\frac{F_M^{\left(\frac{1}{3}\right)}}{U_A^{\left(\frac{2}{3}\right)}}\right] \times X^{\left(\frac{1}{3}\right)} \geq 0 \qquad \textbf{equation 3.10.1}$$

or

$$\Delta H_M = K_M \times \left[\frac{F_M^{\left(\frac{1}{3}\right)}}{U_A^{\left(\frac{1}{3}\right)}}\right] \times t^{\left(\frac{1}{3}\right)} \geq 0 \qquad \textbf{equation 3.10.2}$$

where $F_M = \dfrac{\rho_O \times U_O^{\,2} \times r_O^{\,2}}{\rho_A}$ = momentum parameter **eq 3.11**

K_M = momentum constant $= \mathbf{2.3}$ $(Briggs)$

For many vents jets and those flares categorized by **inertia dominance**, the momentum component at source is significant and can be observed to be contributory to overall flame size. Whilst there is an unresolved question about how this momentum may be conserved or destroyed by the normal flame turbulence, this model assumes that the initial momentum in the stream is conserved as the flame develops. This component is essentially similar to that condition utilized by the API RP-521 "simple" model.

3.5 LOW VELOCITY ABERRATIONS

The current model, so far, has been primarily concerned with higher flow rates and velocities and the wind velocity anomalies of the Majeski model are not fully predicted by the algorithm in its basic form.

When wind flows across vertical cylinders, such as flare stacks, a slight positive stagnation pressure occurs on the windward face. Air flowing around the stack accelerates slightly as it might across an aerofoil and this produces a slight depression in pressure in the wind shadow area, due to the Bernoulli principle. The maximum magnitude of the pressure differential across the diameter can be roughly two times (2x) the normal stagnation pressure of the wind speed.
Gases discharged from the stack with little upward momentum can be forced into the negative pressure zone in a demonstration of downwash.
Thus, the following correction is suggested to allow for the differential effects of the negative pressure zone generated behind the stack by the wind, and the stagnation pressure on the windward side

$$U_{O1} = [U_O - (1.4 \times U_A)] \quad \text{= corrected discharge velocity} \qquad \textbf{equation 3.12}$$

The corrected value, U_{O1}, would be used in determination of F_B, and F_M, in earlier formulae.
Clearly, when $U_A \geq 0.7 \times U_O$, U_{O1} will become negative and demonstrate downwash, which is the defining characteristic of flames categorized by **wake dominance**.

The effect of any down wash condition will be to slightly delay the commencement of thermal rise.

The maximum extent of downwash is un-documented for flames and, even allowing the use of a directional vector, the Briggs formula will not predict a downwash condition. In order to allow a mathematical solution, a tentative modeling approach is suggested as 5 diameters adjusted by the relative relationship of the downwash effect to the modified exit velocity such that

downwash = $$\Delta H_D = 5 \times D_S \times \frac{U_{O1}}{1.4 \times U_{AS}} \leq 0$$ **equation 3.13**

where U_{AS} = wind speed at the top of the stack.

This produces a representative effect reducing to zero as the discharge velocity increases.

Wind-induced turbulent wakes can form behind cylindrical objects for a range of wind speeds[12] even exceeding a Reynolds number ($\mathscr{Re}$) of 200,000, which extends well into a range of moderate wind speeds for vertical flare stacks.

$\mathscr{Re}$ = dimensionless Reynolds Number $= \dfrac{U_A \times D_S \times \rho_A}{\mu_A}$ **eq 3.14**

where D_S = stack/flare tip outside diameter

μ_A = viscosity of air

Although not addressed by the Gogolek characterizations, an additional, and readily observable features of many large wind-blown flames is a tendency for the flames formed from gases with a low discharge velocity to split into two distinct tails. This effect is sometimes, although not always, accompanied by some downwash on the leeward side of the flare.

The effect is due to interactions between complex shear forces and vortices in the tilting plume at the point of discharge with the well known, *von Karman*[13], vortices which form on the back-side of the flare. These vortices are themselves generated by the interaction of the negative pressure zone in the wind shadow of the flare stack cylinder and the dynamic movement of the air flow around the cylinder. The effect is most commonly experienced as the structural design factor of potential wind-induced (vortex shedding) vibrations of the stack and the associated use of spiral vortex breakers.

Two tornado-like spirals of air occur just behind the flare stack which can influence the motion of gases leaving the tip and within close proximity of these vortices. The effect is most noticeable when the tip exit velocity is very low. The two "tails" can each be seen as rolling cylinders with their downward-facing surfaces moving transverse to the flame centerline in a pattern known as a counter-rotating vortex pair (CVP). The atmospheric conditions which generate this effect most strongly depend on the wind speed and the stack diameter and would seem to be most probable in a range of Reynolds number ($\mathscr{Re}$) between 30 and 5000 corresponding to very light winds.

The two (CVP) "tails" are sometimes sufficiently distinct to be considered as two independent flames. Such a double flame effect will clearly influence the location of the flame "center" for radiant purposes, bringing it closer to both the flare and grade. In addition below the flame, the two tails can each contribute equally to radiant heat at grade, making the low velocity case somewhat more severe than the current single source models might suggest.

Accordingly, for these conditions, the following additional modification is suggested for calculation of flame conditions in each tail

$$t_{FMOD} \quad \text{= modified dwell time} \quad = 0.5 \times q_F \times \left(\frac{K_S}{K_F \times U_A^{(1+N)}} \right)^{\left(\frac{1}{N}\right)} \qquad \textbf{eq 3.15}$$

This modification would be reflected in the overall formula for downwind flame travel and the associated plume rise.

At some condition of increase in wind and U_{O1} this approach results in a discontinuity, at which point the flame should redevelop as a single entity although it may still develop as a "wake". This jump has neither been investigated nor proven but it does not seem to be an unreasonable supposition. With increases in discharge velocity, the rise would eventually revert to the original formulae.

4 EVALUATING PRACTICAL CONSTANTS

4.1 TURNER DISPERSION COEFFICIENTS

The equations developed so far have been dimensionless and need to be resolved in consistent units. A number of constants are not evaluated as they depend on the units used in the calculation. For these, the following guidelines are offered.

Using conventional dispersion coefficients as a basis we can estimate initial, trial values for the two constants N and S by interpolation of Turner's published dispersion factors σ_Y and σ_Z.

for near-field conditions	Category A	Category B	Category C	Category D
Dispersion constant - S				
X_F in metres	0.0390	0.0387	0.0250	0.0108
X_F in feet	0.0390	0.0459	0.0318	0.0142
Dispersion exponent - N	2.0016	1.858	1.7973	1.7727

The variations in the exponent N reflect differences in the plume flattening which occurs downwind for the different stability categories. In the close field, flame location, and for all stability categories it is probably satisfactory to evaluate N as $N_T = 2$ which allows consistency of units and implies a notionally conical expansion of gases into the flame zone.

This generates a small error in S based on the published values for the various stability categories, which already vary significantly.
As needed, an alternative estimate for a corrected S_X in any category may be made from the formula

$$S_X = S \times (downwind\ travel)^{(N-2)} \qquad \textbf{equation 4.1}$$

Unfortunately, this correction requires an iterative aspect to the calculation procedure, but is easily accomplished with modern computing techniques.
When establishing basic design conditions, it is probably satisfactory to anticipate the neutral stability Category "D".

When calculating F_H, selections of a value for Cp depends to some extent on the particular section of the plume under consideration.

- in the far field (plume strongly diluted by air) Cp_A (specific heat of air) is appropriate.
- within the flame, Cp_O (specific heat of discharge) is more valid, even though this will transition to the specific heat of the flue gas as the flame proceeds.

It is also significant to bear in mind that wind speed varies with height and surface drag conditions. Conventionally, winds are specified at a given height above grade. At other elevations it is suggested to use a standard wind height correction such as that provided in ASCE-7[14] and noted below.

$$U_{AH} = U_A \times \left(\frac{H}{H_O} \right)^{\Phi} \qquad \textbf{equation 4.2}$$

where H = height in consideration
H_O = ref height for wind speed (most commonly 10 metres above grade)
Φ = wind height exponent according to terrain [varies from 1/5 to 1/11]

For consistency, the downwind distance to a modified value of S_X should coincide with the mid flame (or mid-plume) height used for the wind speed in the various prior formulae.

4.2 COMPARISON WITH OTHER MODELS

To examine the model, the prior formula for ΔH_F has been compared with available field data, published data and the two, common flame models in API RP-521. The series of comparative graphs appended to this paper show flame shapes developed by this model (BUO), the Brzustowski model (BRZ) and the API "simple" (API) model. The conditions for each investigation are shown with each curve and all represent specific points plotted in RP-521 Figs 8 and 9.
Very little data is provided with the API-521 flame length plot and a variety of assumptions have been made for each data point in order to facilitate a complete calculation. The variables needed for the models but not provided in RP-521 have been interpreted from the associated text and are all shown in the figures.

Despite the need for assumptions, the new formulae appear to tie in fairly well to the available data for observed flames over a representative range of wind speeds. Similarities between the API simple curve and the BUO curves appear in moderate wind conditions but the models show differences in flame length at some wind speeds. The BRZ model does not readily concur with either the BOU model or the pattern of flames lengths of RP-521 Fig 8. These differences in the BRZ model highlight this author's concerns about the overall suitability of the widely used BRZ model for flare design.

4.3 PRACTICAL FIELD OBSERVATIONS

Practical readings of flame length taken in the field tend to be very subjective. Even if dimensions are accurately determined, the recorded conditions will rarely include a complete profile that includes all of the relevant stability conditions and included flows.

4.3.1 INCLUDED FLOWS AND GAS CHARACTERISTICS

In most locations where flare flame length is of interest, and may be recorded, the gases being burned will probably be hydrocarbons which, if burned unassisted, will make smoke. Operation with an unnecessarily smoky flame during field readings is not a preferred mode of operation and it is quite possible that readings of flame length will be made on a clean flame, which is subjected to steam injection and is thus unrepresentative relative to the basic model.
To make some accommodation for this factor, the additional materials in the flame (steam or air) need to be recorded and the adjusted value for C_L and CV allowed in the calculation of K_F.

Shore[15] provides an approach to assessment of C_L, for mixtures which include inert gases such as steam, which may be beneficial in this matter. This will not include the influence of additional injection-based turbulence on the flame length. For a practical recording with a clean steam-injected flame, reduce the steam to the minimum tolerable to permit a "just clean" flame, before taking readings.

4.3.2 ESTIMATING THE STABILITY CONDITION

Atmospheric stability is extremely variable and dependent on many environmental factors. For the BUO model, it also has significant influence on the flame shape. A nomograph (figure 6) has been prepared for the purpose of stability category estimation in the field, based on the descriptive texts of Turner and Briggs and the Solar radiation model of Bird and Hustrom[16]

5 THE PROCEDURE

5.1 CONVENTIONAL, VERTICAL FLARE DISCHARGES

At the end-of-flame location X_F, for conventional vertical flares, the model and calculation procedure resolve to

a) determine the flow characteristics for the discharged gas $[q_F, CV, \rho_O, C_L, U_O, \varepsilon]$

b) determine the physical characteristics of the flare $[H_S, D_S, r_o]$

c) determine the atmospheric reference conditions $[Stability, S, N, U_A, T_A, \rho_A, Cp_A, \Phi, H_O]$

d) estimate or calculate corrected values of

$$U_{AS} = U_A \times \left(\frac{H_S}{H_O}\right)^{\Phi} \quad \text{for } H_S = \text{stack height} \qquad \textbf{eq 4.2.1}$$

$$U_{AC} = U_A \times \left(\frac{H_C}{H_O}\right)^{\Phi} \quad \text{for } H_C = \text{mid flame height} \qquad \textbf{eq 4.2.2}$$

X_C = downwind distance to mid flame

$$S_X = S \times X_C^{(N-2)} \qquad \textbf{eq 4.1}$$

$$K_B = 1.6$$

$$K_M = 2.3$$

$$K_S = \frac{1}{2 \times \pi \times S_X} \qquad \textbf{eq 2.5}$$

$$K_F = CV \times \rho_O \times C_L \qquad \textbf{eq 2.4}$$

$$t_F = \left[\frac{q_F \times K_S}{K_F \times U_{AC}{}^3} \right]^{\left(\frac{1}{2}\right)} \qquad \textbf{eq 2.6}$$

$$X_F = U_{AC} \times t_F \qquad \textbf{eq 2.7.1}$$

$$U_O = \frac{q_F}{CV \times \rho_O \times \pi \times r_o{}^2} \qquad \textbf{eq 5.1}$$

$$U_{O1} = U_O - (1.4 \times U_{AS}) \qquad \textbf{eq 3.12}$$

$$F_F = \left[\frac{g}{\pi \times Cp_O \times T_A \times \rho_A} \right] \times \left[1 - (1.5 \times \varepsilon) \right] \qquad \textbf{eq 3.7}$$

$$F_M = \left(\frac{\rho_O}{\rho_A} \right) \times U_{O1}{}^2 \times r_o{}^2 \qquad \textbf{eq 3.11}$$

$$\Delta H_M = K_M \times \frac{F_M{}^{\left(\frac{1}{3}\right)}}{U_{AC}{}^{\left(\frac{2}{3}\right)}} \times X_F{}^{\left(\frac{1}{3}\right)} \qquad = 0 \ \textit{if} \ U_{O1} \le 0 \qquad \textbf{eq 3.10}$$

$$\Delta H_D = 5 \times D_S \times \left(\frac{1.4 \times U_{AS}}{U_{O1}} \right) \le 0 \qquad \textbf{eq 3.13}$$

$$\Delta H_{F1} = 0.5 \times K_B \times \frac{\left(F_F \times q_F\right)^{\left(\frac{1}{3}\right)}}{U_{AC}} \times X_F{}^{\left(\frac{2}{3}\right)} \qquad \textbf{eq 3.1}$$

$$\Delta H_F = \Delta H_{F1} + \Delta H_M + \Delta H_D \quad = \text{rise at flame end} \qquad \textbf{eq 5.2}$$

e) determine the intermediate mid flame locus $[H_C ; X_C]$ and iterate to convergence.

Throughout this analysis, the Zero wind condition is clearly an asymptote requiring an alternative treatment. This condition is not discussed in this paper and requires additional investigation. A limiting minimum wind speed of 1 fps (0.3 m/s) is suggested for calculations involving low wind speeds

By substitution for U_O in the calculation of F_M, the formula may be rearranged into the form

$$\Delta H_F = \frac{q_F{}^{0.333}}{A''} + \frac{q_F{}^{0.667}}{B''} \qquad \textbf{eq 5.2.1}$$

where A'' and B'' are complex values including gas composition and velocity.

This solution shows a modest similarity to the common, logarithmic (straight line) solution of RP-521 fig 8

Flame length = $L_F = \frac{Q_F^{0.467}}{135}$ ft **eq 5.3**

Heat release = $Q_F = 3600 \times q_F$ Btu/h

5.2 A THREE-DIMENSIONAL MODEL

The need for a three-dimensional model is a main reason for the original development of this BUO model, and inclusion of momentum in the algorithm makes this possible.

For the three dimension solution, the basic formula must be divided into the two main components

a ***buoyant*** (thermal or density based) component which is ***always in the vertical direction***

$\Delta Z_T = \Delta H_P = \Delta H_{P1}$ *or* ΔH_{P2} *or* ΔH_{P3}

a ***momentum*** component which is ***axial*** with the discharge

$\Delta \bar{A}_M$ replaces ΔH_M to indicate the vectored result of the axial displacement

The computation is performed most easily using time based formulae rather than distance based formulae and with vectored wind conditions as indicated below and illustrated in the attached figure 7.

The following convention is suggested for representation of coordinates

the angled discharge is	at angle αt to the vertical		
the angled discharge always	points ***towards*** the 0.0 degree plan reference angle		
angles are referenced	from 0.0 degrees, clockwise in plan		
wind blows	***from*** orientation	αw	
	towards orientation	$\beta w = \alpha w + 180$	degrees
X	= axial / horizontal direction/ distance	+ ve values towards 0 degrees	
Y	= cross axis / transverse direction / distance	+ ve values right of 0 degrees	
Z	= vertical direction / distance	+ ve values upward	

cross discharge wind $U_{AO} = U_{AS} \times \sqrt{(\sin(\beta w))^2 + (\cos(\beta w) + \cos(\alpha t))^2}$ **eq 5.4**

cross axis wind $U_{AY} = U_{AS} \times \sin(\beta w)$ **eq 5.5**

axial direction horizontal wind $U_{AX} = U_{AS} \times \cos(\beta w)$ **eq 5.6**

turbulence adjusted discharge $U_{O2} = U_O + (U_{AX} \times \sin(\alpha t))$ **eq 5.7**

downwash-corrected discharge $U_{O1} = U_{O2} - (1.4 \times U_{AO})$ **eq 5.8**

the downwash correction is applied to the *axial* direction.

$$\Delta H_{F1} = 0.5 \times K_B \times \left(F_F \times \frac{K_F}{K_S} \right)^{\left(\frac{1}{3}\right)} \times U_{AF}^{\left(\frac{2}{3}\right)} \times t^{\left(\frac{4}{3}\right)} \qquad \textbf{equation 3.1.5}$$

$$\Delta \overline{A}_M = K_M \times \left(\frac{F_M}{U_{AY}} \right)^{\left(\frac{1}{3}\right)} \times t^{\left(\frac{1}{3}\right)} \qquad \textbf{equation 5.9}$$

using constants and derived values as previously defined.

Plotting the flame (or downwind plume) centerline locus becomes a simple solution of vectored values based on the defined X; Y; Z axes.

All momentum-based travel is related to the discharge axis direction X

Vertical momentum travel = $\Delta Z_M = \Delta \overline{A}_M \times \cos(\alpha t)$ **equation 5.10**

Horizontal momentum travel = $\Delta X_M = \Delta \overline{A}_M \times \sin(\alpha t)$ **equation 5.11**

Total along-axis travel = $\Delta X = \Delta X_M + (U_{AX} \times t)$ **equation 5.12**

Cross-axis travel = $\Delta Y = U_{AY} \times t$ **equation 5.13**

Rise = $\Delta Z = \Delta Z_M + \Delta Z_T$ **equation 5.14**

6 THE DOWNWIND PLUMES

6.1 THE OVERALL PLUME TRAJECTORY

This model allows the standard plume formulae to be used in the down stream zone such that, during the plume rise section beyond the end of the flame, the actual rise is reduced by a fixed quantity equal to the rise difference between the end of the flame and the fully developed plume at the same downwind distance. From the prior analyses, it is clear that the end-of-flame thermal rise is one half (1/2) of the normal plume thermal rise at the flame end distance.

The ability to generate a plume trajectory in the downwind near-field location of the flame, is not normally significant in plume calculations, when the overall objective is to determine ground level concentrations. In these cases, the theory relies on a plume which has already reached its final height and distributes, in a Gaussian manner, into the atmosphere.
For these cases, the normal governing stability categories should be used, with appropriate selection of dispersion coefficients.

The total plume rise to a horizontal condition is generally accepted to be limited by atmospheric turbulence. The height and distance limits for the maximum rise vary with stability condition. For stable and neutral conditions a range of down wind distances to a level plume is given by various authorities. Beychok[17], and others provide a formula based on the Buoyancy parameter F_B.

$$X_{FINAL} = 119 \times F_B^{0.4} \text{ metres} \qquad \text{for units of } F_B \text{ given in } m^4/s^3 \qquad \textbf{eq 6.1}$$

This applies for values of $F_B \geq 55$ $m^4.s^{-3,}$ which corresponds to thermal sources in excess of roughly 5.9 MW (or 20 million Btu/h), covering most flaring conditions.
For a hot source F_B is replaced by $F_H \times q$ and for a flame source F_B is replaced by $F_F \times q_F$.

For these distant field calculations, when final rise is limited as indicated, any height corrections due to the initial flame position will become insignificant to the final height of the plume.

6.2 CONCENTRATIONS IN THE DISTANT FIELD

In the distant field, for calculations of ground level concentration, plume reflection at the ground is a factor and the dispersion formula is expressed as

$$\chi_1 = \frac{1}{2 \times \pi \times \sigma y \times \sigma z \times U_A} \times \exp\left\{\frac{-1}{2} \times \left(\frac{Y}{\sigma y}\right)^2\right\} \times \left\{\exp\left[\frac{-1}{2} \times \left(\frac{H-Z}{\sigma z}\right)^2\right] + \exp\left[\frac{-1}{2} \times \left(\frac{H+Z}{\sigma z}\right)^2\right]\right\} \times T_W$$

equation 6.2

where χ_1 = an eigenvalue for the specific property or pollutant to be investigated
H = vertical elevation of plume centerline
Y = horizontal transverse distance from the plume centerline
Z = vertical distance from the plume centerline

σy = horizontal dispersion coefficient for the relevant stability and distance

σz = vertical dispersion coefficient for the relevant stability and distance

T_W = time weighting multiplier (see below)

Published horizontal and vertical dispersion coefficients are, generally, based on empirical results and are related to a specific sampling time. The limits set on ambient pollutant concentration are generally referred to as the REL (recommended exposure limit). These are also given as a TWA (time weighted average). When evaluating the probable downwind ground level concentration of pollutants from any source, including a flare, care must be taken to adjust the calculation in such a manner as to coordinate the time base of the dispersion coefficients with that of the REL. Turner gives an approximation of the relationship as

$$T_W = \left[\frac{\textit{averaging time of coefficient}}{\textit{required averaging time}} \right]^{(0.17)} \qquad \textbf{equation 6.3}$$

Thus, dispersion values predicted using dispersion coefficients obtained from 10 minute sampling, are slightly higher than those appropriate for comparison with a typical OSHA TWA based on a 15 minute sample and should be reduced by the appropriate T_W

6.3 NEAR-FIELD PLUME PROPERTIES

When dealing with flares, often, a near-field estimate of plume trajectory is needed to assess whether a hot plume from the flame is likely to impact another piece of equipment, such as another flare, a tall distillation column or personnel access areas, and, if so, under what conditions and degree of severity. Application of the BUO model, with the height correction beyond the flame makes this possible.

Because plume dilution occurs from the moment the flame commences, at the point of discharge, the standard dispersion coefficients should apply. As with the prior development of the flame dwell-time relationship, the important characteristics lie on the plume centerline, and the same simplifications should be practical for the down stream near-field, such that

$$\chi_1 = \frac{1}{\pi \times 2 \times \sigma y \times \sigma z \times U_A} \qquad \textbf{equation 2.1.1}$$

$$\chi_1 = \frac{1}{\pi \times 2 \times S_X \times X^2 \times U_A} \qquad \textbf{equation 2.1.2}$$

where X = downwind distance

Most of the estimations needed in the near field represent a physical condition which may present an immediate hazard to personnel. For such cases, the subjective response of exposed personnel cannot, reasonably, be averaged over a 10 or 15 minute exposure time and a 3 second exposure would probably be a more appropriate sample time. Accordingly, using the prior time adjustment formula, a multiplier of T_W = 2.5 should be applied to the eigenvalue χ_1 for these conditions when possible personnel exposure is involved.

Applying this technique to the flame we find that

Plume Temperature (above ambient) $$= \chi_1 \times T_W \times (1 - 1.5 \times \varepsilon) \times \frac{q_F}{Cp_A \times \rho_A}$$ **eq 6.4.1**

With substitution of the prior relationship for downwind distance at the flame end, it can easily be seen that this yields a flame end temperature that corresponds to the flame temperature at the lean limit, without the application of the factor T_W. However, this is such an obviously dangerous location and high temperature that downwind investigations will not normally be performed. Further down wind the 2.5 multiplier introduced by T_W can be seen to represent a realistic factor of safety. Additional analysis yields a rule of thumb that plume temperatures may be intolerable for a downwind distance of roughly 20 flame lengths.

Unburned gas concentration $$= \chi_1 \times T_W \times w_O \times \left(\frac{100 - \eta}{100} \right) \text{ [M.L}^{-3}\text{]}$$ **eq 6.4.2**

$$= \chi_1 \times T_W \times \frac{w_O}{\rho_O} \times (100 - \eta) \times 1{,}000{,}000 \text{ [ppm]}$$ **eq 6.4.3**

where w_O = pollutant output rate into the flame

η = destruction efficiency in flame

Flue gas concentration

Down wind flue gas concentration depends on the rate of flue gas production, which in turn depends on the original gas composition. Where this can be determined, and a flow rate calculated, downwind concentrations are calculated directly from the eigenvalue

$$= \chi_1 \times T_W \times w_F \text{ [M.L}^{-3}\text{]}$$ **eq 6.4.4**

where output of Flue Gas = $w_F = R_F \times w_O$ **eq 6.5**

R_F = Mass Ratio of Flue gas to flammable component

If the gas composition is not known in sufficient detail to determine a value for R_F, a reasonably accurate estimate may be made by "rule of thumb", based on the heat release. It is usually possible to obtain a first order estimate of flue gas rate (+/- 20%) from

$$w_F = \frac{q_F}{K_{R1}} \qquad \textbf{equation 6.6}$$

applying a representative flue gas MW = 28 downwind,

this yields a concentration of flue gas $\approx \chi_1 \times T_W \times \frac{q_F}{K_{R1}}$ [M.L^{-3}] **equation 6.4.5**

where K_{R1} = 1200 Btu/lb ~ 667 kcal/kg

or a Vol Concentration of Flue Gas $V_F \approx \chi_1 \times T_W \times q_F \times K_{R2}$ % vol **equation 6.7**

where K_{R2} = 1.13 % / Btu ~ 0.285 % / kcal

Oxygen concentration is determined directly from the flue gas concentration such that

$$V_{OX} = 0.21 \times (100 - V_F) \quad \% \text{ vol} \qquad \textbf{equation 6.8}$$

A breathable concentration needs to be greater than 19.5 % Oxygen. Substitution of previous results suggests that a minimum of 5 clear flame lengths is necessary to avoid oxygen deficit. Given the, earlier, similar finding that 20 clear flame lengths may be necessary to avoid high flue temperatures, it seems elevated temperature can serve as an adequate warning to personnel to escape from an engulfing plume of flue gas. Of course, this must be tempered by knowledge of any other, potentially harmful constituents of the plume.

For a non-vertical tip, the locus of the near field, downwind plume is offset from the wind line through the tip discharge according to the offset formulae previously outlined for the three-dimensional flame itself. As with a vertical tip, the vertical thermal rise can be calculated from the normal plume rise formulae with the appropriate adjustment for the flame end rise.

6.4 RADIANT CENTER

Although the main purpose of this model is to define conditions other than the radiant output of the flame, the nature of the model is such that it may posibly be used for Radiant predictions in the same manner as the API and BRZ models previously discussed. At this time, no investigations have been performed which suggest a departure from the common, point source spherical model., although preliminary review of photographic evidence strongly indicates a common flame shape, predictable using equation 6.9.

Based on the flame residence time formula of this paper, as the gas burns within the flame, and the heat release develops to fraction j, the downwind travel relationship can be adjusted accordingly.

$$X_J = \sqrt{j \times qF \times \frac{KS}{K_F \times U_A}} \qquad \textbf{equation 2.7.2}$$

One possible measure of the center of the flame occurs when 50% of the gas has been consumed, at $j = 0.5$ such that $X_C \approx 0.7 \times X_F$ or 70% of the downwind flame length. ΔH_C or ΔZ_C as required may be calculated using the previous formulae with appropriate substitution of X_C.

An alternative approach to radiant center may be derived from the same distribution pattern used for the initial development of the flame model which develops as a relationship for

flame radius parameter $R = \sqrt{-2 \times {\sigma_R}^2 \times \ln\left\{\chi \times 2 \times \pi \times {\sigma_R}^2\right\}}$ **equation 6.9**

where ${\sigma_R}^2 = S_X \times X^2$ **equation 6.10**

using previously defined parameters.

Plume radius calculated from this formula needs an additional multiplier to incorporate the volume expansion due to high temperature, in order to generate a meaningful flame shape.
This approach, when integrated, together with photographic evidence, suggests a “pseudo-spherical” center at roughly 60% of the flame length and is probably the most realistic practical selection. More formula development is required, however, before the appropriate flame emissivity (or radiated fraction) can be adequately related to this flame shape or the equivalent radiant sphere.

7 FLAME EFFICIENCY

An interesting aspect of the flame "dwell time" model is a possible tie-in to flame efficiency predictions.

Johnson et.al[18] suggested that there exists a relationship of $U_A / U_O^{1/3}$ which allows prediction of flame inefficiency. Their text suggests that efficiency improves with heat content of the flammable material but is independent of total heat release. However, an alternative treatment may yield an alternative conclusion.

Rearranging the limited data published in the Johnson paper allows all the curves to be redrafted, with good accuracy, in the form

$$100 - \eta_C = K_1 \times \exp\left\{ K_2 \times \left[\frac{U_A}{U_O^{1/3}} \right]^{(3/2)} \right\} \qquad \textbf{equation 7.1}$$

Interpolated data from the Johnson paper is compared with this formula in the enclosed graph figure 8.

This, can be expressed using a re-arrangement of the prior formula for t_F, such that

$$t_F^{\,2} = \frac{r_O^{\,2}}{2 \times S \times C_L} \times \frac{U_O}{U_A^{\,3}} \qquad \textbf{equation 2.6.2}$$

or

$$\sqrt{\frac{U_O}{U_A^{\,3}}} = \frac{t_F}{r_O} \times \sqrt{2 \times S \times C_L} \qquad \textbf{equation 2.6.3}$$

leading to

$$100 - \eta_C = K_1 \times \exp\left\{ \frac{-K_T}{t_F} \right\} \qquad \textbf{equation 7.2}$$

which is the well known form for growth and decay relationships, in which the effective basis is the theoretical residence time of the flame reaction given by the BUO formula. The values for K_1 and K_T shown here as constants, will undoubtedly prove to be a functions of the other physical characteristics of the system and are clearly targets for further research.

Factors already in evidence, which may influence the overall equation include the jet size, the lean limit concentration of the fuel mixture and the stability parameter S. For the small-scale Johnson work in a wind tunnel the neutral case is suggested.

Other factors may include a measure of the initial rate of conversion at the commencement of the flame (t = 0), or the superficial rate of regression, which would suggest an involvement of the component reactivity as discussed previously.

This possible link with efficiency is a very significant finding as it predicts high conversion efficiencies for those conditions which would exist during field-testing, and during which high conversion efficiencies have been practically determined. It also leads to a conclusion of high conversion efficiency for the emergency design cases, which are the bases of most elevated flare designs. However, it raises the possibility of very poor efficiencies for the majority of industrial flares when operating on low-load, which is the common, day-to-day condition. The potential significance of this possible relationship mandates more testing before the formula can be applied as anything other than an estimate.

8 CONCLUSION

The author recognizes that this has been, primarily, a theoretical, mathematical analysis and that many of the ideas introduced may conflict with current calculation procedures and furthermore, that in some ways, the model may raise more questions than it answers. However, in addition to the mathematical arguments expounded in the forgoing, the analyses are also based on the author's personal observations and experience over many years of dealing with combustion and flares. The overall aim has been to produce generally more useful algorithms than those in common use at this time.

As a result of this approach it has been possible to bring together many separate elements of flare flame and plume analysis. This complete model generates information which may be used, together with other standard methods, to estimate

- flame positions for any direction of discharge or wind
- flare flame size and "center" location for radiant heat calculations
- flame centerline and plume locus for near field impact studies
- plume centerline locus for far field pollutant concentration studies
- flame residence time for estimations of component destruction efficiency
- flame residence/wind relationships for estimations of component combustion efficiency
- the specific disruptive effects of down-wash in the lee of the flare tip.

As far as practical, the results of this analysis have been cross referenced against field results but others are strongly encouraged to generate field data or specific research analyses for additional

cross references, in all areas of the extended models covered by this paper. If desired, such data may be submitted to the author for this purpose.

CAUTION

The reader is cautioned that calculations for downwind pollutant REL may be subject to regulatory approval and that Regulatory Authorities may require calculations to be performed according to a specific protocol. This treatise is not intended to supplant those methods for distant field calculations but simply to highlight the effects in the local plume and provide a means of estimating often-overlooked, near-field values.

ACKNOWLEDGEMENTS

The author wishes to thank the Management of Flaregas Corporation for facilitating the preparation and presentation of this paper, and the AIChE Session Chairman for his assistance with editing and formatting the final presentation.

The AUTHOR

David SHORE has made a number of presentations on Flaring to A.I.Ch.E,, other major Institutions and Corporate Bodies. He has been involved with Combustion and Flare Design since 1965 and is employed as the Chief Engineer of Flaregas Corporation in New York, U.S.A. Mr. Shore is a frequent contributor to Engineering Fora, and maintains a web site dedicated to consultancy on technical issues of Combustion and Flaring.

FIGURES

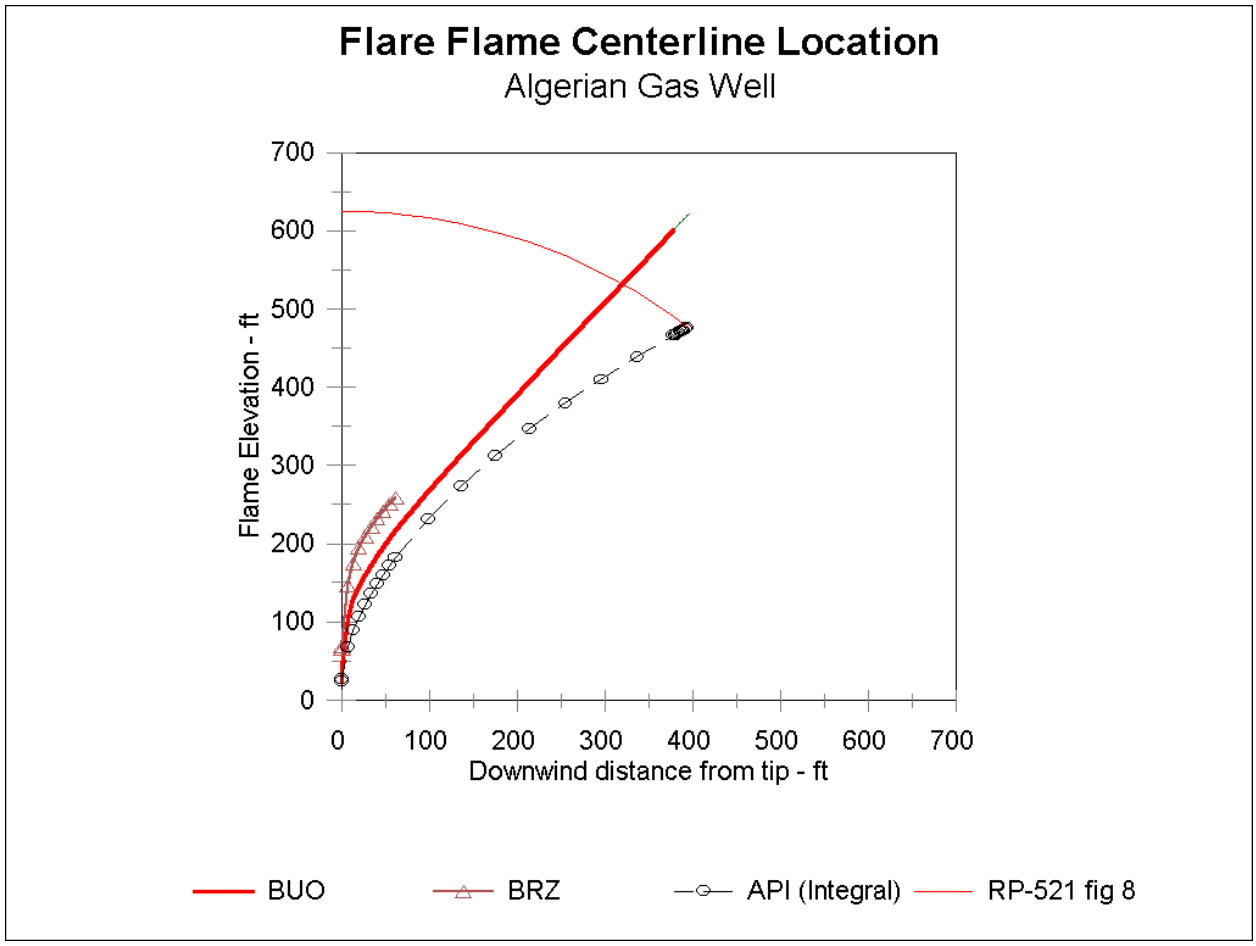

Figure 1 - Calculated Flame Pattern / Algerian gas Well

Derived and Estimated Values for Flame Position Calculations - Ref API-521 Fig 8					
Flow Rate	2,000,000 lb/h	Wind Speed	18 fps	RP-521 Length	600 ft
Mol Weight	23.9	Solar Contrib	370 Btu/sq.ft_h	BRZ Length	268 ft
Temperature	150 deg F	Stability	C	BRZ Rise	238 ft
Calorific Value	20160 Btu/lb	Flare Height	25 ft	BRZ Travel	66 ft
LEL	4 %			API Length	664 ft
Total Heat	4.0E+10 Btu/h	BUO Rise	576 ft	API Rise	444 ft
Flare Dia	42“	BUO Travel	378 ft	API Travel	383 ft

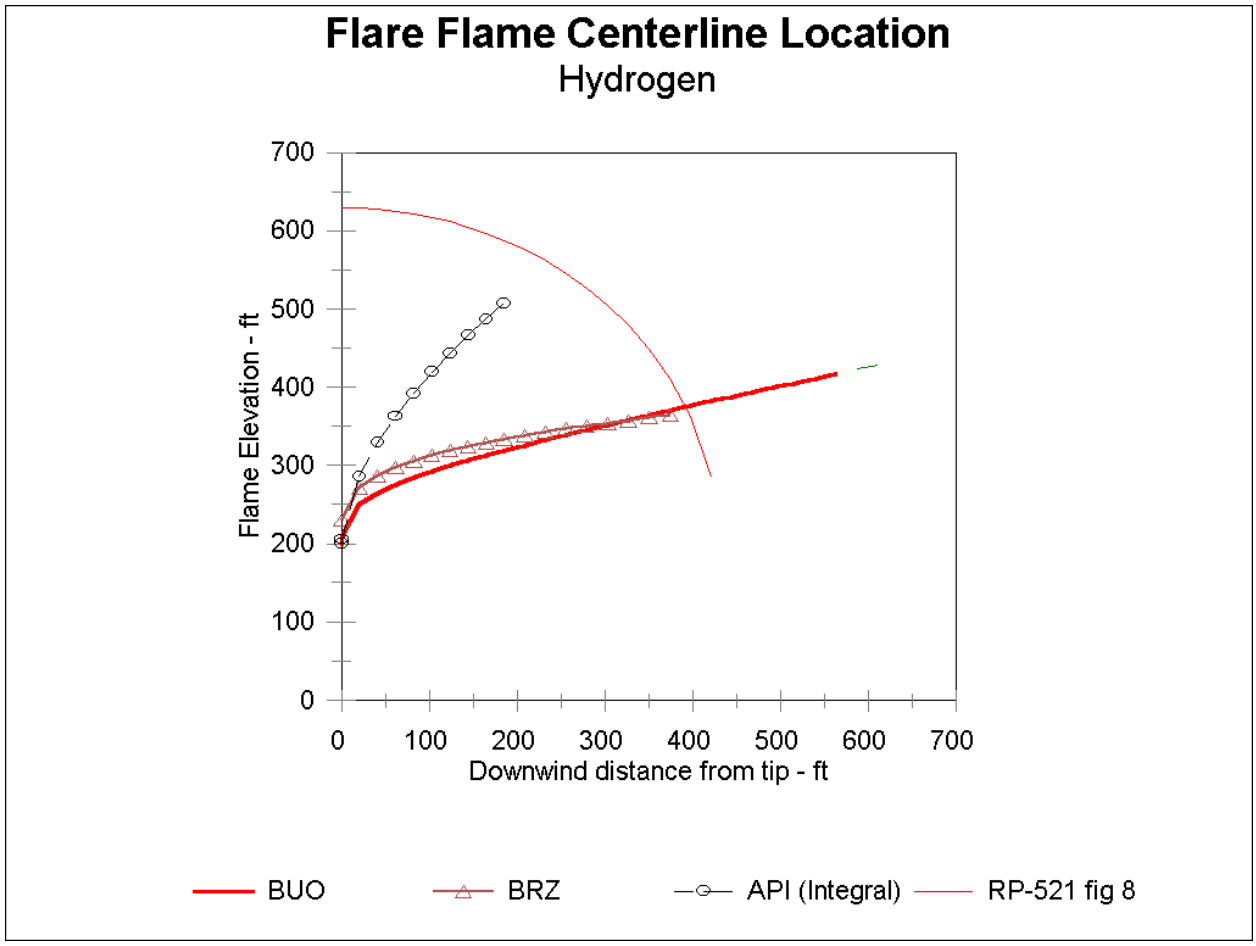

Figure 2 - Calculated flame Pattern / Hydrogen Flare

Derived and Estimated Values for Flame Position Calculations - Ref API-521 Fig 8					
Flow Rate	280,000 lb/h	Wind Speed	40 fps	RP-521 Length	430 ft
Mol Weight	2	Solar Contrib	250 Btu/sq.ft_h	BRZ Length	453 ft
Temperature	200 deg F	Stability	D	BRZ Rise	165 ft
Calorific Value	51625 Btu/lb	Flare Height	200 ft	BRZ Travel	381 ft
LEL	4 %			API Length	412 ft
Total Heat	1.45E+10 Btu/h	BUO Rise	218 ft	API Rise	314 ft
Flare Dia	30“	BUO Travel	564 ft	API Travel	192 ft

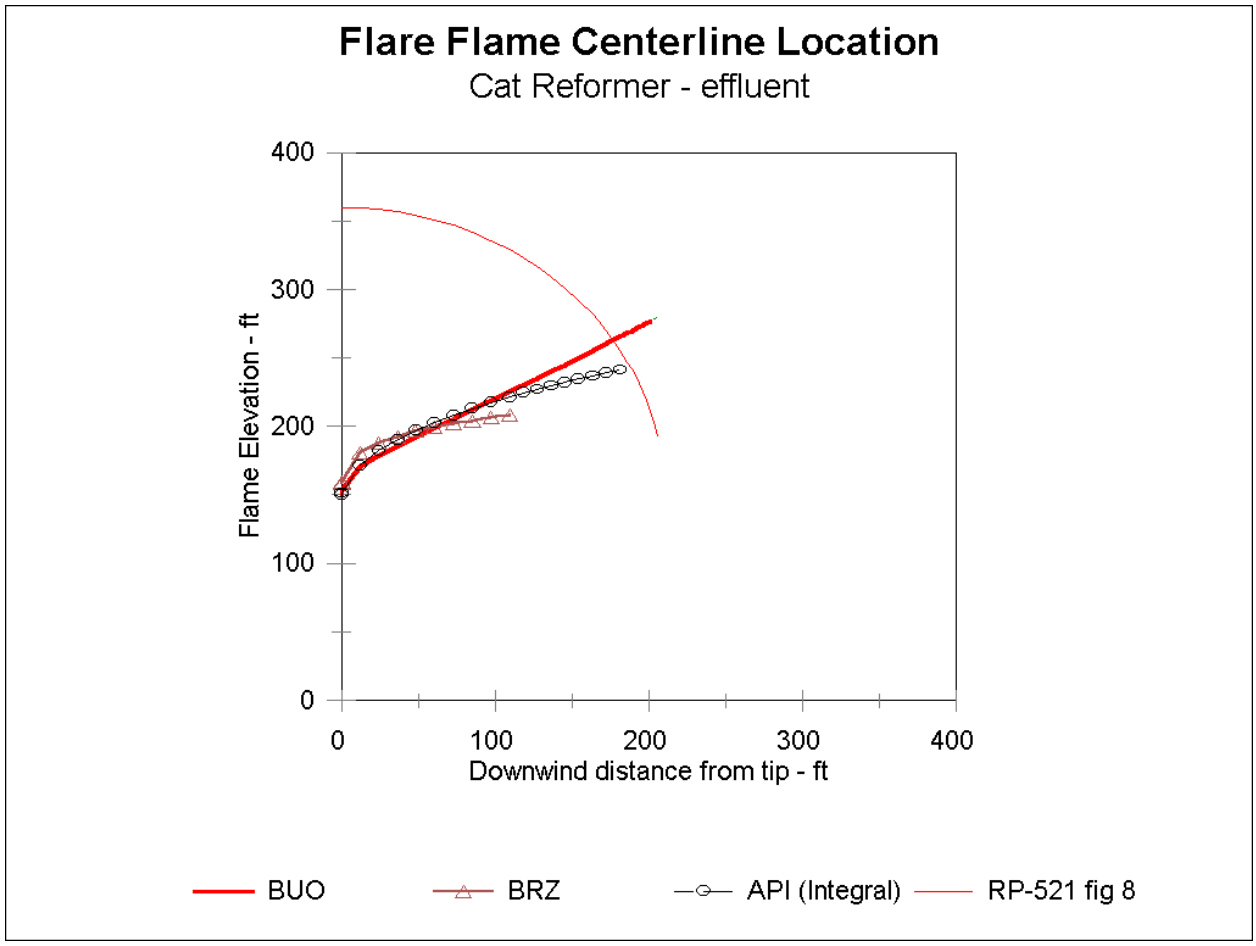

Figure 3..- Calculated flame Pattern / Catalytic Reformer Effluent

Derived and Estimated Values for Flame Position Calculations - Ref API-521 Fig 8					
Flow Rate	200,000 lb/h	Wind Speed	20 fps	RP-521 Length	210 ft
Mol Weight	59.4	Solar Contrib	250 Btu/sq.ft_h	BRZ Length	138 ft
Temperature	350 deg F	Stability	D	BRZ Rise	59 ft
Calorific Value	19620 Btu/lb	Flare Height	150 ft	BRZ Travel	110 ft
LEL	1.7 %			API Length	224 ft
Total Heat	3.9E+9 Btu/h	BUO Rise	127 ft	API Rise	91 ft
Flare Dia	24“	BUO Travel	201 ft	API Travel	180 ft

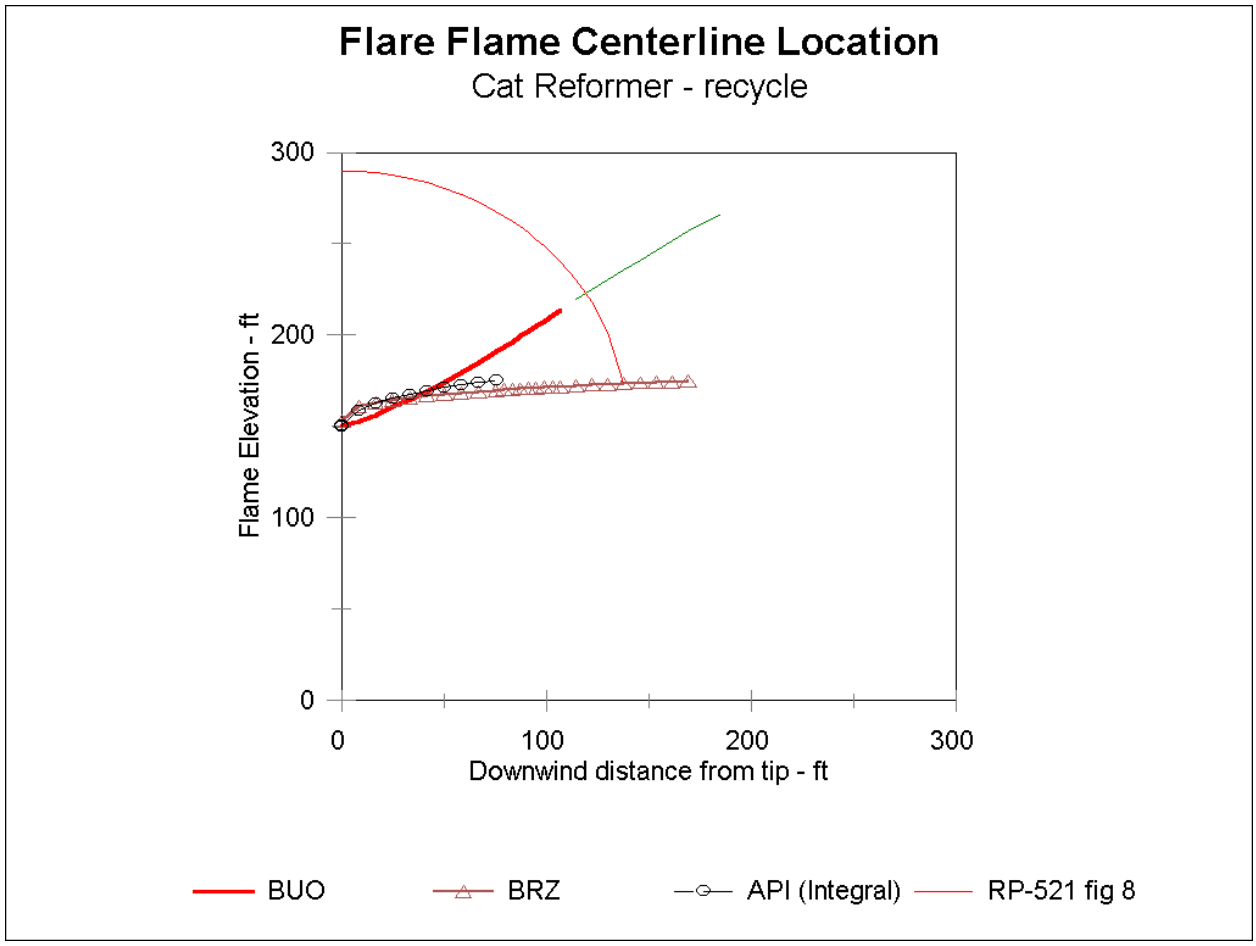

Figure 4 - Calculated flame pattern / Catalytic Reformer Recycle gas

Derived and Estimated Values for Flame Position Calculations - Ref API-521 Fig 8					
Flow Rate	26,000 lb/h	Wind Speed	8 fps	RP-521 Length	140 ft
Mol Weight	97.4	Solar Contrib	250 Btu/sq.ft_h	BRZ Length	173 ft
Temperature	350 deg F	Stability	D	BRZ Rise	25 ft
Calorific Value	19225 Btu/lb	Flare Height	150 ft	BRZ Travel	166 ft
LEL	1.1 %			API Length	86 ft
Total Heat	5.0E+8 Btu/h	BUO Rise	64 ft	API Rise	25 ft
Flare Dia	24“	BUO Travel	107 ft	API Travel	75 ft

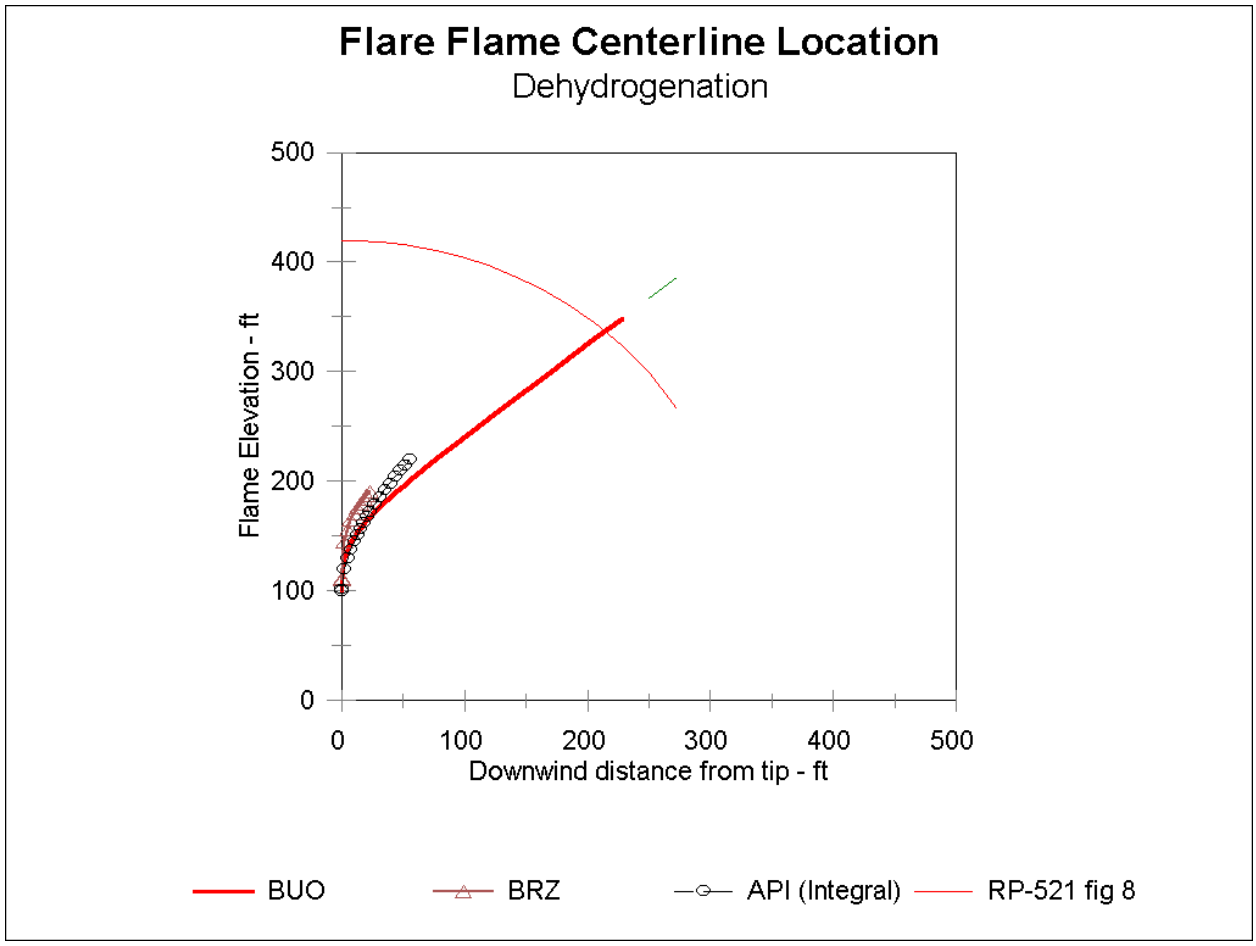

Figure 5 - Calculated Flame pattern / dehydrogenation unit

Derived and Estimated Values for Flame Position Calculations - Ref API-521 Fig 8					
Flow Rate	80,000 lb/h	Wind Speed	10 fps	RP-521 Length	320 ft
Mol Weight	11.3	Solar Contrib	250 Btu/sq.ft_h	BRZ Length	100 ft
Temperature	200 deg F	Stability	D	BRZ Rise	91 ft
Calorific Value	19700 Btu/lb	Flare Height	100 ft	BRZ Travel	24 ft
LEL	4.4 %			API Length	146 ft
Total Heat	1.6E+9 Btu/h	BUO Rise	249 ft	API Rise	120 ft
Flare Dia	12“	BUO Travel	228 ft	API Travel	56 ft

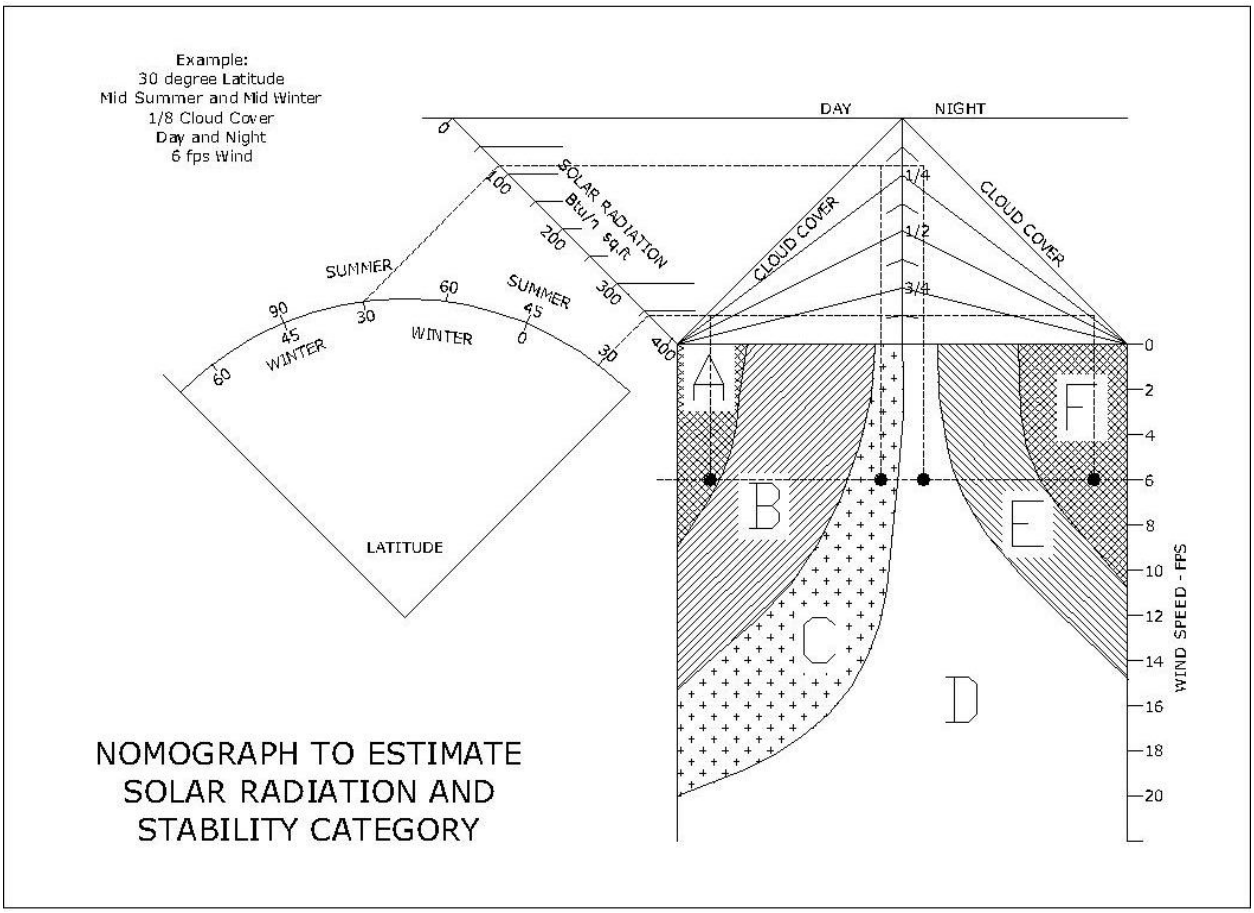

Figure 6 - Nomograph to Estimate Solar Conditions and Stability Categories

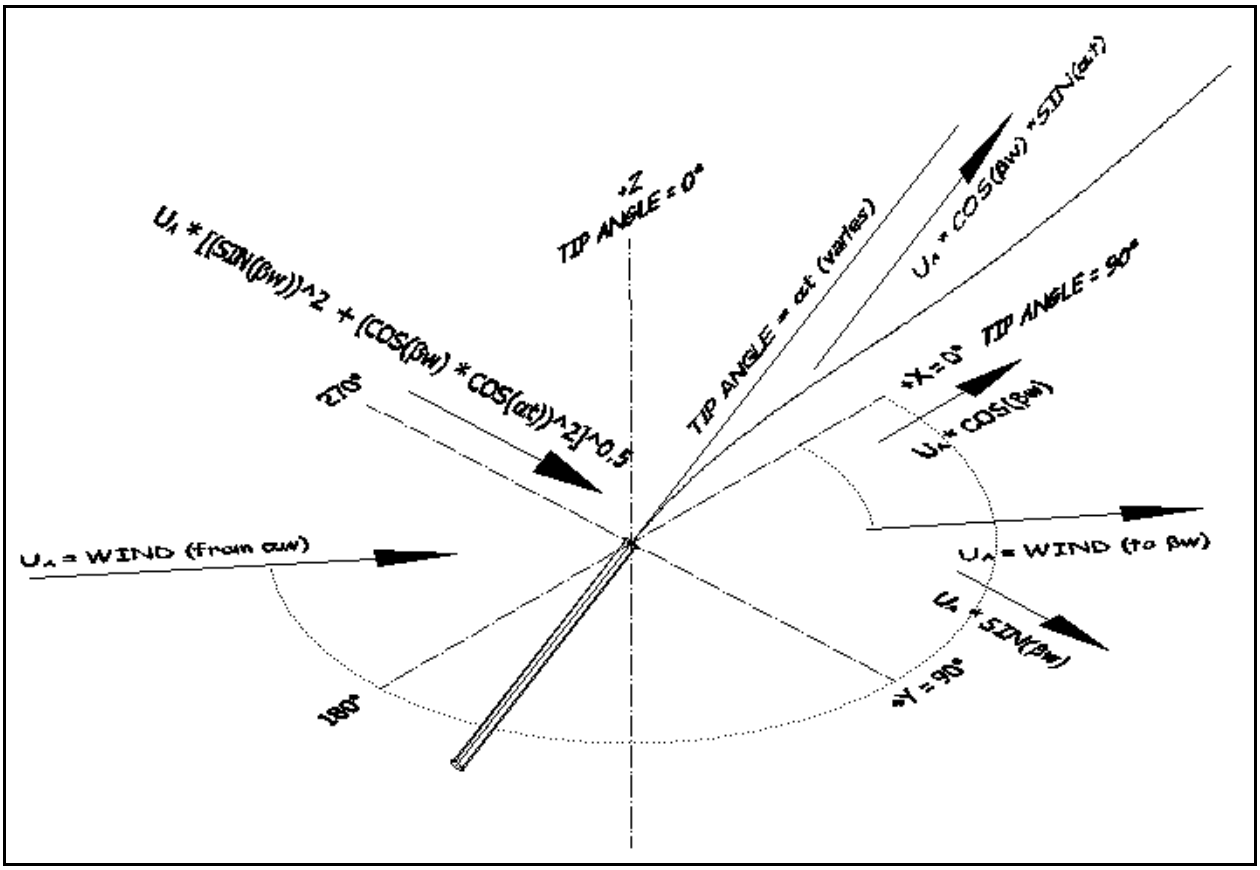

Figure 7 - Directional Conventions for Three Dimensional Flame Model

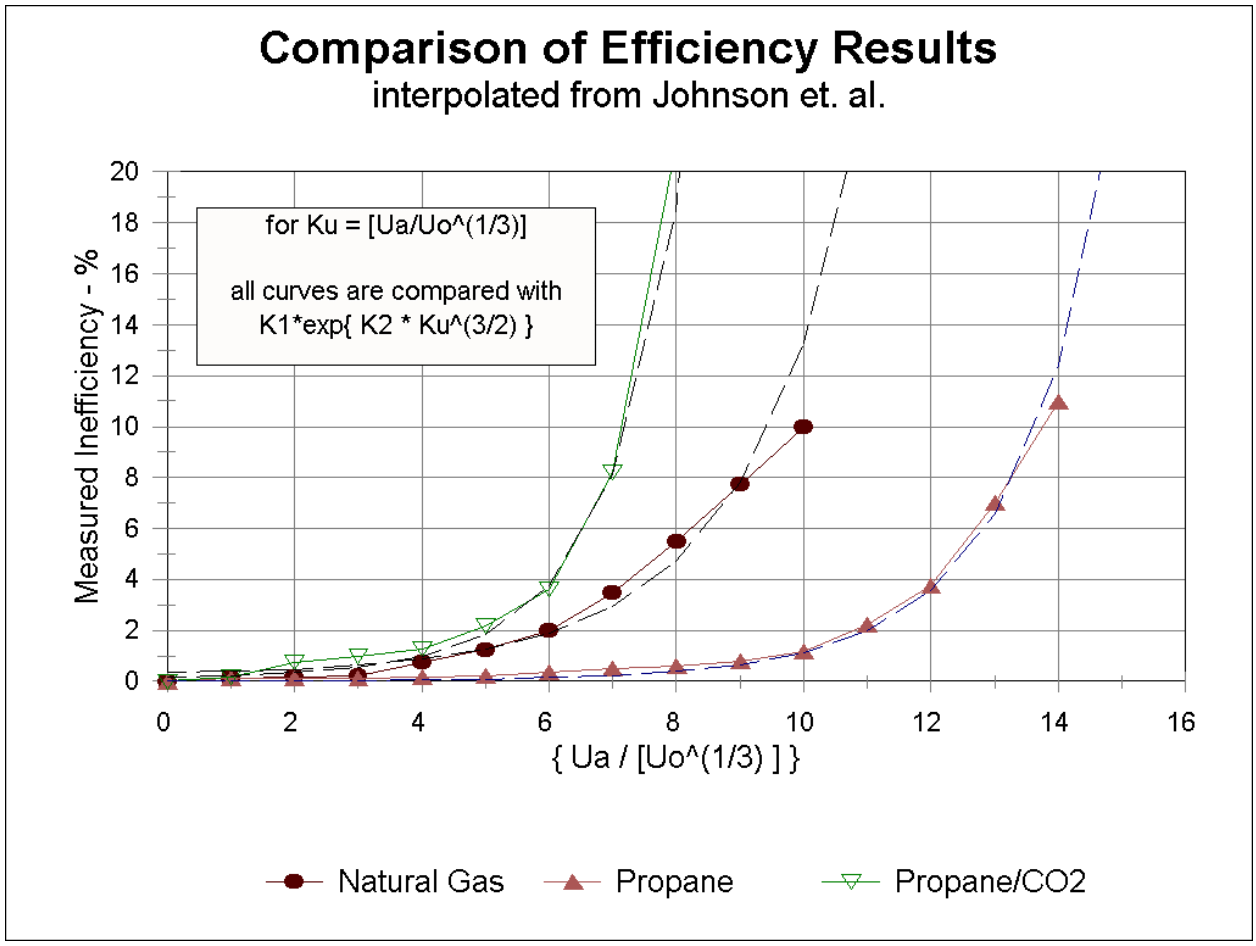

Figure 8 - Combustion Inefficiency for small jet in Wind Tunnel

BIBLIOGRAPHY

1 *Recommended Practice RP-521; Guide for Pressure-Relieving and Depressuring Systems*; American Petroleum Institute, Washington. D.C.

2 Brzustowski, T.A., & Sommer, E.C. Jr.; "Predicting Radiant Heating from Flares"; *Proceedings – Division of Refining*, Volume 53, pp 865-893; American Petroleum Institute, Washington. D.C; 1973.

3 Majeski, A.J., Wilson, D.J.& Kostiuk, L.W.; "Local maximum Flame Lengths of Flares in a Crosswind"; Combustion Inst (Canadian section); May 1999.

4 Hottel. V.O., & Luce, R.G.; "Burning in Laminar and Turbulent Fuel Jets"; *Fourth Symp (intl) on Combustion*; the Combustion Institute; 1953.

5 Zukoski, E.E.; "Scaling Flame lengths of Large Diffusion Flames"; National Institute of Standards and Technology, Annual Conference on Fire Research; pp 39-40; 1996.

6 Gogolek, P.E.G. & Hayden, A.C.S.; "Wind Turbulence and Elevated Flare Flames", Presentation to the American Flame Research Committee, 2004.

7 Pasquill, F.; "The Estimation of the Dispersion of wind borne material"; Meteorol Mag. 90, 1063, 33-49, 1961.

8 Gifford, F.A.; Atmospheric Dispersion calculations using the generalized Gaussian Plume model", Nuclear safety, 2, 2, 56-59, 67-68, 1962

9 Turner. D.B.; "Workbook of Atmospheric Dispersion Estimates"; U.S. Dept of Health, Education & Welfare, 1967

10 Pohl. J.H., Payne. R., and Lee.J; "Evaluation of the Efficiency of Industrial Flares"; U.S. Environmental Protection Agency; EPA-600 / 2-84-095

11 Briggs. G.A.; "Plume Rise"; U.S. Atomic Energy Commision, 1969

12 Simiu. E. and Scanlon R.H.; "Wind Effects on Structures"; Wiley-Interscience Publications, 1978

13 Von Karman, T.; "Über den Mechanismus des Widerstandes den ein bewegter Körper in einer Flüssigkeit efährt"; Nachrichten der Könglichen Gesellschaft der Wissenschaften, 1911.

14 ASCE-7-98; "Minimum Design Loads for Buildings and Structures"; A.S.C.E (publ 1998)
[Issues of ASCE-7 which post-date 1998 are available with more complex height exponents but which are more applicable to structural design. Appropriate terrain characteristics should be interpreted per the code parameters.].

15 Shore.D; "Making the Flare Safe"; A.I.Ch.E, Proceedings of 30th Loss Prevention Symposium, Paper 12d. 1996.

16 Bird. R.E. and Hulstrom. R.L.; "A Simplified Clear Sky model for Direct and Diffuse Insolation on Horizontal Surfaces" . Solar Energy Research Institute, Golden, Co; SERI Technical Report SERI/TR-642-761, Feb 1991

17 Beychok, M.R.; "Fundamentals Of Stack Gas Dispersion", published by the author, fourth edition, 2005.

18 Johnson. M.R., Zastavniul. O., Wilson. D.J. and Kostiuk. L.W.; "The Combustion Efficiency of jet Diffusion Flames in Cross-flow"; Presentation to The Combustion Institute, Washington D.C.; March 15-17, 1999.